

Cross-Control of Magnetization and Polarization by Electric and Magnetic Fields with Competing Multiferroic and Weak-Ferromagnetic Phases

Y. J. Choi, C. L. Zhang,* N. Lee, and S-W. Cheong

*Rutgers Center for Emergent Materials and Department of Physics and Astronomy, Rutgers University,
136 Frelinghuysen Road, Piscataway, New Jersey 08854, USA*

(Received 19 January 2010; published 23 August 2010)

From our investigation of magnetoelectric properties of a multiferroic phase in $\text{Eu}_{0.75}\text{Y}_{0.25}\text{MnO}_3$ competing with a weak-ferromagnetic phase in magnetic fields, we found intriguing hysteretic behaviors of physical properties with variation of temperature and magnetic field. These hysteretic behaviors arise from the kinetic arrest (dearrest) processes of the first-order multiferroic-weak-ferromagnetic transition, resulting in frozen (melted) magnetoelectric glass states with coexisting two phases. Tipping the delicate balance of two competing phases by applying electric and magnetic fields leads to a remarkable control of magnetization and electric polarization.

DOI: 10.1103/PhysRevLett.105.097201

PACS numbers: 75.85.+t, 75.30.Kz, 77.80.-e

Coexistence of two or more distinct physical phases in complex materials, where various physical degrees of freedoms are intricately coupled and a number of order parameters are delicately balanced, is associated with a variety of unprecedented physical phenomena [1–3]. For instance, in perovskite manganites, the delicate balance between localization and hopping of charge carriers induces the competition of ferromagnetic (FM) metallic and antiferromagnetic (AFM) charge-ordered-insulating phases [1,4]. This competition can, in turn, lead to the coexistence of those two phases at low temperatures (T), formed by kinetic arrest of the first-order AFM-insulating to FM-metallic transition [5–7]. The formation of the magnetic glass depends sensitively on external perturbations such as strain or applied magnetic fields (H) [6,8], which is closely related to the origin of the colossal magnetoresistance effect of perovskite manganites [1,4]. Evidently, scientific understanding of the interrelationship between the nanoscale coexistence of competing phases and macroscopic physical properties is crucial for controlling the functionality of complex materials.

Multiferroics, where magnetism and ferroelectricity coexist in one material, have attracted great interest due to remarkable cross-coupling effects between seemingly distinct physical properties [9,10]. In a new class of multiferroics called magnetism-driven ferroelectrics, magnetic order without space-inversion symmetry breaks lattice space-inversion symmetry through exchange striction, inducing ferroelectricity [9,10]. Sufficient external H can change the spin configuration of magnetic order in magnetism-driven ferroelectrics and can result in drastic changes of ferroelectric (FE) and dielectric properties, i.e., large magnetoelectric (ME) effects [11–14]. Herein, we present a new way of achieving a colossal ME effect in a multiferroic by utilizing the high sensitivity of competing magnetic phases to external perturbations. We found that, in $\text{Eu}_{0.75}\text{Y}_{0.25}\text{MnO}_3$, a multiferroic (MF) phase with a cycloidal-spiral magnetic state can exist simultaneously

with a weak-ferromagnetic (WFM) phase in H . A glasslike ME state, called a ME glass, forms at low T by the kinetic arrest of the first-order spiral magnetic to WFM transition, resulting from the retarded growth of the low- T WFM phase out of the supercooled high- T MF phase upon cooling [5,6]. Upon heating, the ME glass becomes dearrested to the equilibrium WFM phase via thermal fluctuations above the freezing T [5,6]. Dynamically modulated two phases exhibit fascinating T -dependent magnetic and FE behaviors, and magnetization (M) and polarization (P) exhibit highly enhanced responses to electric fields (E) or H .

$\text{Eu}_{1-x}\text{Y}_x\text{MnO}_3$ ($x \leq 0.45$) crystallizes in an orthorhombically distorted perovskite structure (space group $Pbnm$) [15–18]. It is reported that continuous increase of orthorhombic distortion by replacing Eu^{3+} ions by smaller Y^{3+} ions leads to an evolution of low- T ground state from the WFM to the MF phase with a spiral magnetic order [16–18]. For x equal to or near zero, the low- T magnetic state in zero H is a canted A-type AFM phase, i.e., a WFM phase, where Mn spins are aligned ferromagnetically in the ab plane and antiferromagnetically with a slight canting along the c axis [Fig. 1(a)]. Significant structural distortions for large x values result in a spiral spin state within the ab plane, which gives rise to a bulk FE polarization along the a axis, P_a [Fig. 1(b)] [19–21]. A single crystal of $\text{Eu}_{0.75}\text{Y}_{0.25}\text{MnO}_3$ was grown by a floating zone method in argon gas flow. Three types of magnetic and electric measurements were performed: warming measurements after zero H cooling (ZFC-W), cooling measurements in H (FC-C), and warming measurements after cooling in H (FC-W). M was measured with a SQUID magnetometer (Quantum Design MPMS). P and the dielectric constant (ϵ) were obtained by integrating pyroelectric current measured with an electrometer and using an LCR meter at $f = 44$ kHz, respectively [22].

Our single-crystalline $\text{Eu}_{0.75}\text{Y}_{0.25}\text{MnO}_3$ in H exhibits an intricate balance between MF and WFM phases. T -dependent M_c and P_a ($T_{\text{FE}} \approx 30$ K) of $\text{Eu}_{0.75}\text{Y}_{0.25}\text{MnO}_3$

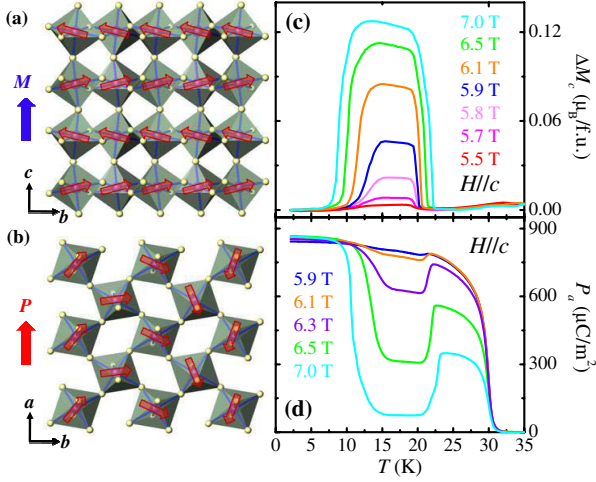


FIG. 1 (color online). (a),(b) Crystallographic and low- T Mn-spin structures of orthorhombic perovskite $\text{Eu}_{1-x}\text{Y}_x\text{MnO}_3$. Magnetic Mn^{3+} ions locate at the center of octahedral O^{2-} cages. Also shown are the directions of M and P of canted A-type AFM (WFM) and cycloidal-spiral magnetic phases, respectively. (c) T dependence of the H_c -induced WFM moment along the c axis, ΔM_c , in $H_c = 5.5\text{--}7.0$ T applied after zero-field cooling. (d) T dependence of P along the a axis, P_a , in $H_c = 5.9\text{--}7.0$ T. Reduction of P_a in intermediate T ranges correlates with the emergence of WFM moment in (c).

[Figs. 1(c) and 1(d)], obtained in ZFC-W in $H_c = 5.5\text{--}7.0$ T, reveal that a WFM moment develops in an intermediate T window in large H_c , and P_a is suppressed when the WFM moment appears. Figure 1(c) shows the T dependence of $\Delta M_c = M_c - \chi_0 H_c$, where linear susceptibility χ_0 is $\sim 0.057 \mu_B/\text{f.u.}$ T (f.u. denotes formula unit) and ΔM_c corresponds to the H_c -induced WFM moment. Note that the maximum WFM moment ($\sim 0.13 \mu_B/\text{f.u.}$) in 7.0 T is comparable with the WFM moment of the canted A-type AFM (or WFM) phase [Fig. 1(a)] in $\text{Eu}_{1-x}\text{Y}_x\text{MnO}_3$ with zero or small x [17,18]. This suggests strongly that in $\text{Eu}_{0.75}\text{Y}_{0.25}\text{MnO}_3$, a WFM phase can appear in large H_c and is energetically nearly degenerate with the persisting MF phase [23]. The intermediate values of ΔM_c and P_a in the T window of $\sim 10\text{--}23$ K in H_c of $\sim 5.5\text{--}7.0$ T suggest the coexistence of MF and WFM phases in a broad phase space region. With increasing H_c , ΔM_c increases, P_a decreases, and the coexisting T region of WFM and MF phases widens.

Detailed magnetic and FE behaviors through different T - H procedures turn out to be consistent with the kinetic arrest and dearrest processes of the first-order MF to WFM transition. These behaviors are closely analogous with the magnetic and transport behaviors of colossal magnetoresistance manganites [6,7,24,25]. Figure 2(a) displays T -dependent ΔM_c obtained through three different T - H procedures in $H_c = 5.9$ T: ZFC-W (open circles), FC-C (open squares), and FC-W (open triangles). The freezing T , T_f , below which kinetics of the first-order MF to WFM transition is arrested probably due to a significant frozen

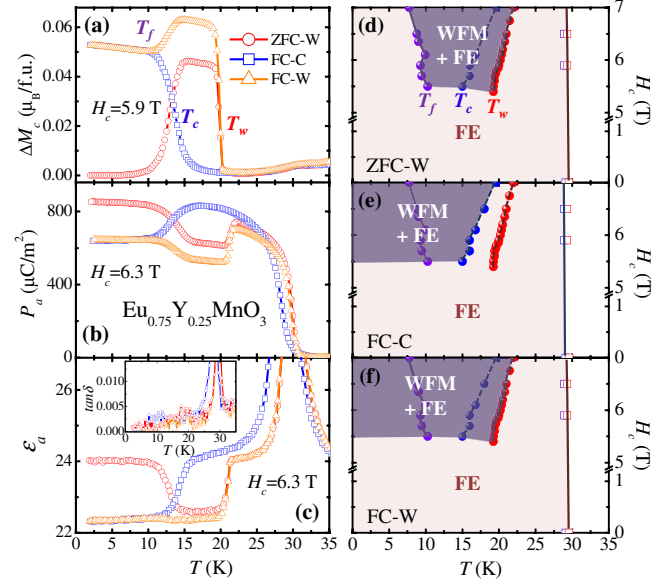


FIG. 2 (color online). (a)–(c) T dependence of ΔM_c in $H_c = 5.9$ T, P_a in $H_c = 6.3$ T, and ε_a [$\tan\delta$ in the inset in (c)] in $H_c = 6.3$ T, respectively. For the data in each figure, three different measurements were performed: upon warming after cooling in $H_c = 0$ T (ZFC-W, open circles), upon cooling in H_c (FC-C, open squares), and upon warming after cooling in H_c (FC-W, open triangles). T_f denotes a freezing T . T_c and T_w correspond to the first-order transition T between the MF and WFM phases for cooling and warming, respectively. (d)–(f) H - T phase diagrams for three different procedures (ZFC-W, FC-C, and FC-W), obtained from T -dependent ΔM_c data. Dark areas represent the coexistence regions of FE and WFM phases, depending on the T - H history.

disorder and thus a ME glass forms, is determined by T at which the FC-C and FC-W ΔM_c curves start to deviate from each other at low T . The first-order nature of the MF to WFM transition is well reflected in the large thermal hysteresis. T_c and T_w denote the transition T upon cooling and warming, respectively. ΔM_c for ZFC-W in $H_c = 5.9$ T is close to zero at low T , indicating that the low- T state after ZFC is purely MF. Upon warming above T_f , the kinetically arrested MF phase starts to get dearrested to the equilibrium state with the coexisting MF and WFM phases. This thermally assisted dearresting process gives rise to a WFM moment upon warming above ~ 10 K [6]. This WFM moment disappears above T_w . For FC-C, a WFM phase develops below T_c and shows an almost plateaulike ΔM_c feature at low T , possibly due to a significantly retarded relaxation below T_f . Upon warming during FC-W above T_f , the frozen ME glass melts, and this melting generates an additional WFM moment upon warming above T_f [24,25].

P_a and ε_a behaviors through different T - H histories are highly consistent with the ΔM_c behavior. For example, P_a in 6.3 T basically behaves in an opposite manner to the variation of ΔM_c [Fig. 2(b)]. Upon warming of ZFC-W, P_a of the MF phase after ZFC decreases in compensation of

the growth of the WFM moment above T_f . At T_w , the reduced P_a jumps to a larger value upon warming while the WFM moment vanishes. P_a for FC-C shows a decrease below T_c in parallel with the emergence of the WFM moment, and the reduced P_a remains intact below T_f . Upon warming of FC-W, the reduced P_a decreases further as an additional WFM moment appears and becomes sharply enhanced above T_w when the WFM phase disappears. ε_a , obtained in 6.3 T [Fig. 2(c)], exhibits a peak at the onset T (~ 30 K) of P_a , similar with a typical behavior at an FE transition. Steplike features of ε_a at T_c and T_w appear similar with those of P_a , and the negligible T dependence of ε_a below T_f is consistent with the formation of a ME glass below T_f through kinetic arrest. The reasonably small magnitude of tangential loss $\tan\delta$ in the inset in Fig. 2(c) indicates that the specimen is insulating enough to sustain the FE properties.

Figures 2(d)–2(f) display T - H phase diagrams from our ΔM_c data for three different procedures in H_c . The phase diagrams manifest coexisting regions of the MF and WFM phases. The MF phase persists below the FE transition T , but the WFM phase appears in different regions, depending on the T - H history. Coexisting T ranges of MF and WFM phases can be summarized as $T_f < T < T_w$ for ZFC-W, $T < T_c$ for FC-C, and $T < T_w$ for FC-W.

We found that magnetic and FE properties of $\text{Eu}_{0.75}\text{Y}_{0.25}\text{MnO}_3$ are controllable by E and H , respectively, through changing the relative volume fraction of the MF and WFM phases. As shown in Figs. 1(c) and 1(d), increasing H_c enhances the WFM phase in the two-phase region while it demotes the MF phase. E_a also considerably influences both phases. In Fig. 3(a), the solid curves show the T -dependent ΔM_c measured in $H_c = 5.9$ T as well as $E_a \approx 10$ kV/cm. It reveals that the WFM moment is remarkably reduced from the value obtained in zero E_a . In ZFC-W, the maximum WFM moment in zero E_a reaches $0.046\mu_B/\text{f.u.}$ at ~ 15 K, whereas the WFM moment in $E_a \approx 10$ kV/cm is reduced by $\sim 50\%$. For the $E_a \approx 10$ kV/cm measurement, E_a was held during the entire process: The initial poling process in $+E_a$ produces a single FE domain with $+P_a$ [22], and warming of the $+P_a$ state in $+E_a$ restrains the development of the WFM moment. Note that, for FC-C and FC-W, the maximum WFM moment was found to decrease by $\sim 30\%$ and 20% , respectively, in $E_a \approx 10$ kV/cm. Note that the T ranges where the WFM moment is significantly influenced by applying E_a match well with the dark shaded regions in the H - T phase diagrams in Figs. 2(d)–2(f), indicating the coexistence regions of the MF and WFM phases. As the WFM moment decreases with E_a , P_a can be “promoted” by applying E_a . Figure 3(b) shows the T -dependent P_a for ZFC-W and FC-W in 6.3 T with and without $E_a \approx 10$ kV/cm. Because of the poling procedure required for the pyroelectric current measurements on $\text{Eu}_{0.75}\text{Y}_{0.25}\text{MnO}_3$, P_a 's with and without E_a begin with the same value at 2 K. P_a curves with and without E_a start

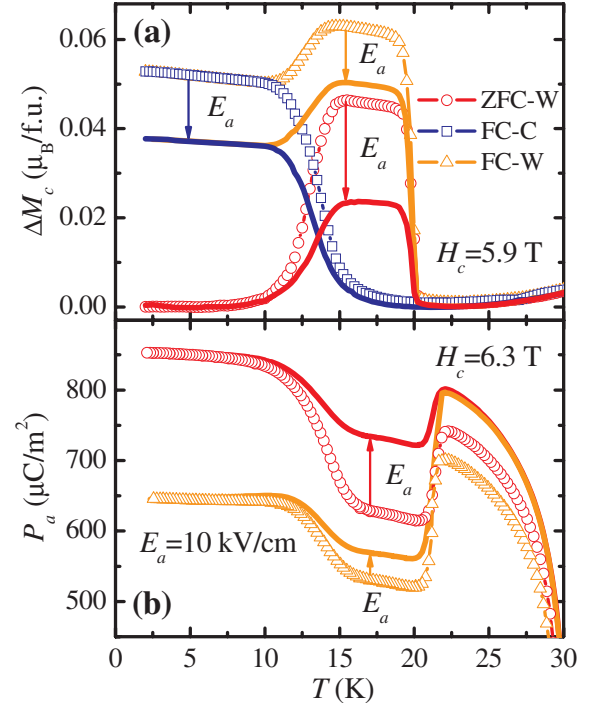


FIG. 3 (color online). (a) Comparison of T -dependent ΔM_c in $H_c = 5.9$ T measured in $E_a = 0$ [the same with the data in Fig. 2(a)] and $E_a \approx +10$ kV/cm (solid curves) for ZFC-W, FC-C, and FC-W. ΔM_c is significantly reduced by the application of E_a in the two-phase coexisting regions. (b) Comparison of T -dependent P_a in $H_c = 6.3$ T in $E_a = 0$ [the same with data in Fig. 2(b)] and $E_a \approx +10$ kV/cm (solid curves) for ZFC-W and FC-W. P_a becomes enhanced with applied E_a in the intermediate T range, where ΔM_c is suppressed with E_a .

to deviate to each other above T_f , and the maximum differences for ZFC-W and FC-W are $\sim 17\%$ and 8% , respectively. The relatively small differences of P_a produced by applying E_a , compared to the ΔM_c differences in Fig. 3(a), may stem from the same poling process used for the P_a measurements with and without E_a . Note that a data set of FC-C is not present in Fig. 3(b) because P_a for FC-C in Fig. 2(b) is obtained always in the presence of poling E_a .

Repeated variation of ΔM_c is achieved by changing E_a linearly between $+10$ and -10 kV/cm as shown in Figs. 4(a) and 4(b). Time-dependent δM_c (the variation of ΔM_c) was measured at 15 K in $E_a = 0$ and $H_c = 5.5$ T, after cooling the specimen in $E_a \approx +10$ kV/cm and $H_c = 0$ down to 2 K and then warming to 15 K in $E_a = 0$ and $H_c = 5.5$ T. Initial poling in $+E_a$ produces a single FE domain with $+P_a$ [22], and warming to 15 K in $H_c = 5.5$ T creates a small WFM moment associated with a small volume fraction of the WFM phase at 15 K. Because of kinetic dearrest at 15 K, ΔM_c relaxes significantly with time as shown in the inset in Fig. 4(a). On top of the relaxation tendency, ΔM_c oscillates in a manner opposite to the variation of E_a . Repeated variation of ΔM_c in Fig. 4(a) is obtained after subtracting the increasing part of ΔM_c as a relaxation background. Initial increase

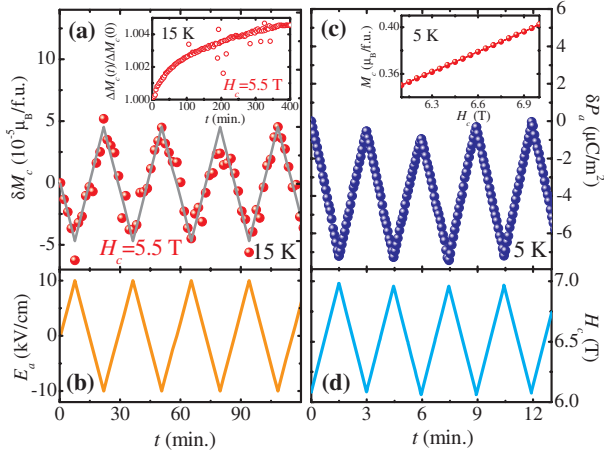


FIG. 4 (color online). (a),(b) Repeated variation of ΔM_c (δM_c) at 15 K in $H_c = 5.5$ T by applying E_a , varied linearly with time between +10 and -10 kV/cm. The inset in (a) shows time-dependent ΔM_c in $H_c = 5.5$ T at 15 K without E_a . δM_c was obtained after subtracting the relaxation part shown in the inset in (a). δM_c follows a linear fit well (solid line) and varies in a manner opposite to the E_a variation, shown in (b). (c), (d) Linearly modulated P_a (δP_a) with time at 5 K with a linear variation of H_c between 6.1 and 7.0 T. The inset in (c) displays H_c -dependent M_c at 5 K for 6.1 T $< H_c < 7.0$ T after cooling in 6.1 T.

of positive E_a leads to a linear decrease in ΔM_c , probably due to strengthening of the MF phase with $+P_a$. When E_a is reduced from +10 and -10 kV/cm, ΔM_c increases linearly. This tendency repeats with oscillating variation of E_a . As a counterpart, modulation of P_a (δP_a) with H_c is obtained at 5 K as shown in Fig. 4(c). Note that, above T_f , the relaxation of P_a (i.e., the continuous decrease of P_a with time) was large, so we were not able to measure the modulation of P_a with H_c . Instead, the specimen was prepared by cooling to 5 K, below T_f , in $E_a \approx +10$ kV/cm and $H_c = 6.1$ T, and then removing E_a . We found that, despite the kinetic arrest below T_f , repeated variation of H_c between 6.1 and 7.0 T [Fig. 4(d)] gives rise to a linear modulation of P_a on the order of 1%, in a manner opposite to the change of M_c [inset in Fig. 4(c)].

In summary, in $\text{Eu}_{0.75}\text{Y}_{0.25}\text{MnO}_3$ with the presence of H_c , a MF phase with cycloidal-spiral magnetism intricately balances with an emergent WFM phase. Coexistence of competing MF and WFM phases in a broad range of T - H phase space results from kinetic arrest-dearrest processes of the first-order MF to WFM phase transition, strongly depending on the T - H history. Coexistence of the competing phases can be significantly influenced by external perturbations such as E and H , which leads to a remarkable control of M and P with E and H . We emphasize that most of the large ME coupling effects in multiferroics are associated with the control of P with H . However, the control

of FM-type M by applying E is most relevant to technological applications, but scarcely observed [26,27]. Our results are clearly distinct from the recent work on GdFeO_3 , where a control of M by E is achieved by manipulating partially clamped FE and FM domains [27], and provide a new revenue to achieve a true cross-control of M and P with E and H .

We acknowledge D. Kwok for improving the presentation of the manuscript. This work was supported by NSF Grant No. DMR-080410.

*Present address: Department of Physics, University of Tennessee, Knoxville, TN 37996, USA.

- [1] See, for example, E. Dagotto, *Nanoscale Phase Separation and Colossal Magnetoresistance* (Springer-Verlag, New York, 2003).
- [2] See, for example, *Proceedings of the Workshop on Phase Separation in Cuprate Superconductors, Erice, Italy, 1992* (World Scientific, New York, 2003).
- [3] R. J. Zeches *et al.*, *Science* **326**, 977 (2009).
- [4] M. Uehara *et al.*, *Nature (London)* **399**, 560 (1999).
- [5] M. K. Chattopadhyay *et al.*, *Phys. Rev. B* **72**, 180401(R) (2005).
- [6] K. Kumar *et al.*, *Phys. Rev. B* **73**, 184435 (2006).
- [7] P. Chaddah *et al.*, *Phys. Rev. B* **77**, 100402(R) (2008).
- [8] K. H. Ahn *et al.*, *Nature (London)* **428**, 401 (2004).
- [9] S-W. Cheong and M. Mostovoy, *Nature Mater.* **6**, 13 (2007).
- [10] D. I. Khomskii, *Physics* **2**, 20 (2009).
- [11] N. Hur *et al.*, *Nature (London)* **429**, 392 (2004); *Phys. Rev. Lett.* **93**, 107207 (2004).
- [12] T. Kimura *et al.*, *Nature (London)* **426**, 55 (2003); *Phys. Rev. Lett.* **94**, 137201 (2005); *Phys. Rev. B* **73**, 220401(R) (2006).
- [13] G. Lawes *et al.*, *Phys. Rev. Lett.* **95**, 087205 (2005); *Phys. Rev. B* **74**, 024413 (2006).
- [14] K. Taniguchi *et al.*, *Phys. Rev. Lett.* **97**, 097203 (2006).
- [15] Y. Noda *et al.*, *J. Appl. Phys.* **99**, 08S905 (2006).
- [16] V. Yu. Ivanov *et al.*, *Phys. Status Solidi B* **243**, 107 (2006).
- [17] J. Hemberger *et al.*, *Phys. Rev. B* **75**, 035118 (2007).
- [18] Y. Yamasaki *et al.*, *Phys. Rev. B* **76**, 184418 (2007).
- [19] T. Kimura *et al.*, *Phys. Rev. B* **68**, 060403(R) (2003).
- [20] H. Katsura *et al.*, *Phys. Rev. Lett.* **95**, 057205 (2005); C. Jia *et al.*, *Phys. Rev. B* **76**, 144424 (2007).
- [21] M. Mostovoy, *Phys. Rev. Lett.* **96**, 067601 (2006).
- [22] See supplementary material at <http://link.aps.org/supplemental/10.1103/PhysRevLett.105.097201> for sample preparation, measurement details, and ferroelectric characterization of $\text{Eu}_{0.75}\text{Y}_{0.25}\text{MnO}_3$ crystal.
- [23] S. Danjoh *et al.*, *Phys. Rev. B* **80**, 180408(R) (2009).
- [24] L. Ghivelder and F. Parisi, *Phys. Rev. B* **71**, 184425 (2005).
- [25] P. A. Sharma *et al.*, *Phys. Rev. B* **71**, 224416 (2005).
- [26] E. Ascher *et al.*, *J. Appl. Phys.* **37**, 1404 (1966).
- [27] Y. Tokunaga *et al.*, *Nature Mater.* **8**, 558 (2009).